CHAPTER III

Deformations of CMP Gathers with $\bar{v}(z)$ To Hyperbolas

3.1. Introduction.

Velocity in the earth varies with depth even when there is strong lateral continuity. In most situations this velocity variation is slow, seismic ray–paths remaining straight for all reflections arriving within cable spread. However, sharp velocity discontinuities near the surface, coupled with long cable spreads, invalidate the small propagation angle requirement for shallow events (vertical two–way traveltime being less than direct arrival to the farthest offest. Schultz, 1980). Because several important seismic data processes, such as hyperbolic velocity estimation and Stolt's imaging, require a near constant velocity wavefield, we introduce a process to deform CMP gathers with some velocity estimate $\bar{v}(z)$ to hyperbolas.

To define the transformation, consider a *Snell trace*. It is defined by all points in a seismic gather that are associated with a fixed *Snell parameter* p. In the particular case when velocity is constant, the Snell trace becomes a straight line with slope $h/t = pv^2$ in time–offset coordinates. We refer to this line as a *radial trace*.

If we transform seismic data for a stratified earth from *Snell trace* space to *radial trace* space, it has the the equivalent effect of mapping non–hyperbolic seismic arrivals into hyperbolic arrivals. The transformation is done in two passes. First we need to get an estimate of the stratified velocity function $\bar{v}(z)$ and transform the data from offset–time coordinates into Snell parameter–depth coordinates. Second we can use a replacement constant velocity $\hat{v}$ and

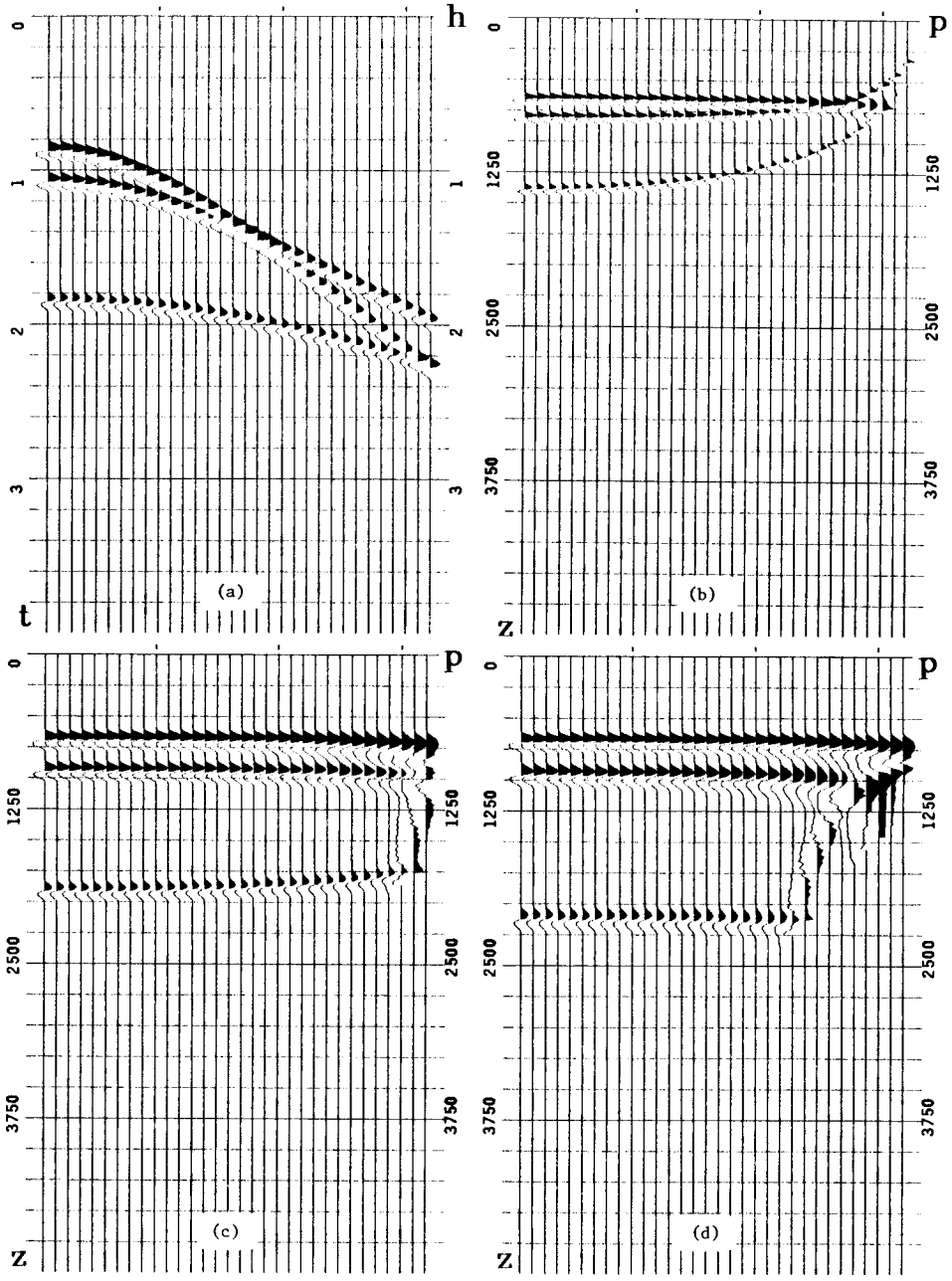

FIGURE 2.1. Mapping to (p, z) space. (a) Synthetic *CMP* gather. (b) Transformation to (p, z) coordinates with constant water velocity, the first reflector has been flattened out. There is a stretch of the wave–form with p, but the first arrivals are independent of p. As expected for the second reflector, we get p–depth dependence. In (c) we have used the correct velocity for the second event. Now arrivals for the first two events are independent of p. There is stretch of the wave–form with depth and the third reflector is curved. In (d) we used the correct velocities for the three reflectors, this has flattened out all the pre–critical reflections. The transformation requires the image at post–critical reflections to become vertical. The p–depth dependence when there are errors in velocity can be exploited to estimate velocity interactively layer by layer.

transform the data from Snell parameter–depth coordinates back to offset–time coordinates. Since the second transformation is done with constant velocity, we can invert the ray equations analytically, with the advantage that the process can be done in a single pass, without need to store an intermediate (p, z) space.

We expect this transformation to be particularly useful in areas where we can predict with certainty a sharp discontinuity in the velocity function, for example the interface between a water layer above and a hard bottom below. The transformation to *radial trace* space will honor Snell's refraction law at the sea–floor–sediment interface. When we do not have good information about the velocity function, the method can be applied iteratively. It will then converge to the true velocity.

3.2. Transformation to (p,z) space with $\bar{v}(z)$.

To define a transformation from stratified to constant velocity wavefields, two steps are needed. First, it is necessary to use an estimate of the velocity function $\bar{v}(z)$ and go to a space where the wavefield depends on depth only. Second, we need to regenerate the original *CMP* geometry (offset–time).

With the ray equations derived in chapter (II), we can define coordinates independent of offset when the exact velocity function is known. A suitable choice is ray–parameter p for lateral coordinate and the depth z.

From chapter (II), the group velocity equations for the exact acoustic wave equation are

$$\frac{dh}{dt} = \frac{pv^2}{2} \tag{2.1a}$$

$$\frac{dz}{dt} = \frac{v(1 - p^2v^2)^{1/2}}{2} \tag{2.1b}$$

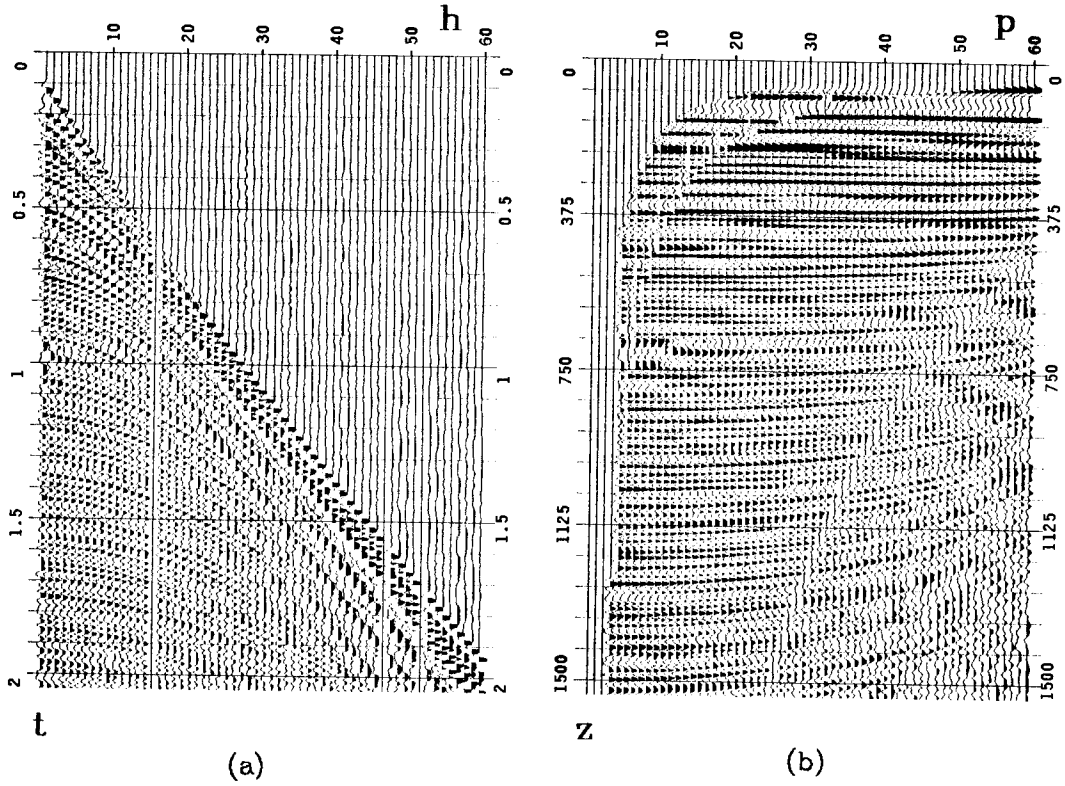

FIGURE 2.2. Marine data in (p,z) coordinates. Constant $\bar{v}$. (a) Marine *CMP* data, square–root gain applied. (b) Transformation to (p,z) space with constant water velocity $v = 1450\ m/sec$. Primaries bend upwards because we are underestimating their velocities. Water multiples appear straight because we used their true velocities, $dp = 8.0 \times 10^{-6}\ s/m$, $dz = 3.0\ m$.

or

$$\frac{dt}{dz} = \frac{2}{v(1 - p^2v^2)^{1/2}} \tag{2.2a}$$

$$\frac{dh}{dz} = \frac{pv}{(1 - p^2v^2)^{1/2}} \tag{2.2b}$$

Integrating equation (2.2) gives the desired transformation equations

$$t = \int_0^z \frac{2\,v(\xi)^{-1}}{\left[1 - p^2 v(\xi)^2\right]^{1/2}} d\xi \tag{2.3a}$$

$$h = \int_0^z \frac{p v(\xi)}{\left[1 - p^2 v(\xi)^2\right]^{1/2}} d\xi \tag{2.3b}$$

It should be noted that there is a limitation in the use of transformation (2.3). When the correct velocity is used, these equations will only flatten *pre−critical* reflections. Refractions and *post−critical* reflections interfere constructively to

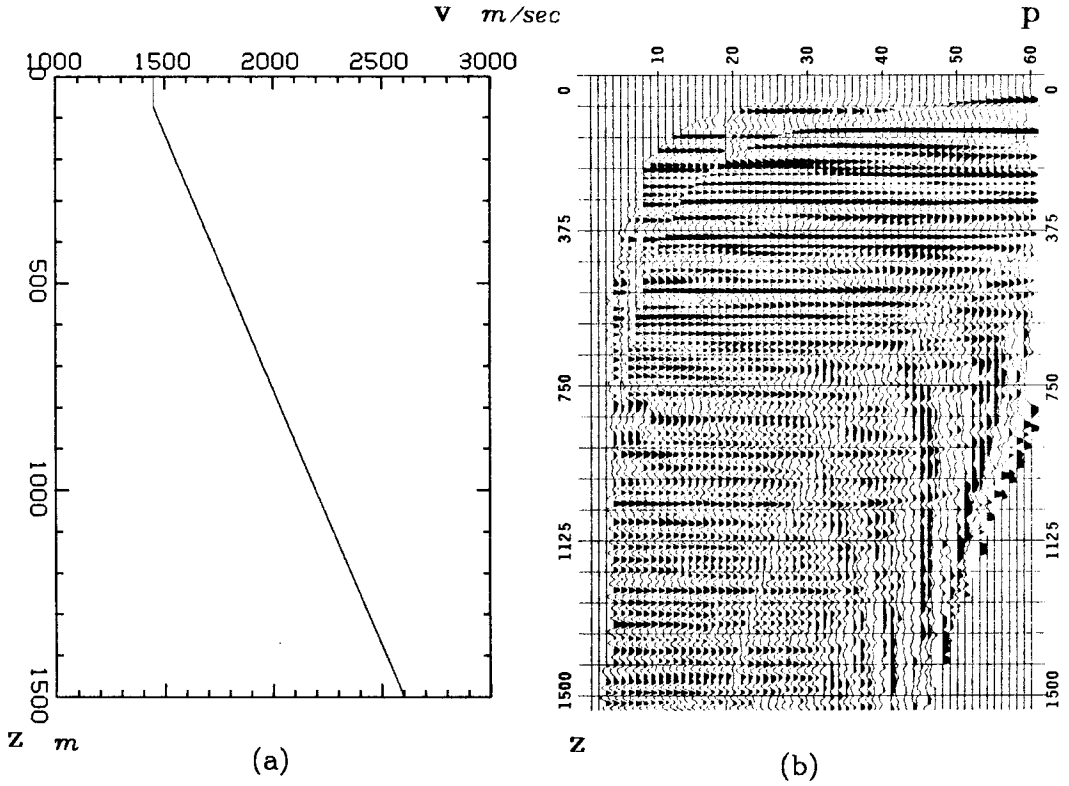

FIGURE 2.3. Marine data in (p,z) coordinates. $\bar{v}(z)$. (a) Velocity function $\bar{v}(z)$. (b) Marine data in (p, z) coordinates transforming with the velocity function (a). Early primary events appear straight, independent of ray−parameter, multiple reflections bend downwards because their depths are overestimated by the velocity function. The effect of overestimation increases with ray−parameter p.

form a $p-z$ image. This image was used by Clayton (1981) to estimate velocity.

In figure (2.1) we display the effect of the transformation (2.3) with a synthetic CMP gather. This is done using exact and perturbed velocities. When velocity is underestimated, there is an increasing error in the estimation of depths with increasing ray–parameter.

In figure (2.2) we display a marine CMP gather and its mapping to (p,z) space using constant water velocity $\bar{v}(z) = 1450\ m/sec$. Sea floor water multiples appear straight, independent of the ray–parameter p. Primary events are curved upwards because we have underestimated their velocities.

Figure (2.3) shows a velocity function $\bar{v}(z)$ and the data into (p,z) coordinates when this velocity function is used. The reference events are now independent of p. Multiples appear to bend downward because we are overestimating their velocities.

It is clear from the examples, that errors in the velocity function $\bar{v}(z)$ will be emphasized near critical angles. Velocity underestimation, for example, will increase depth estimates at wide propagation angles compared to small ones. Only when the correct velocity is used will depth become independent of angle. It is possible to define a velocity estimation process exploiting this sensitivity. This process should determine velocity interactively, one event at a time in chronological order. In the marine case we start with water velocity and flatten the first sea floor reflection. Then we pick the next primary arrival and use its variation of depth with p to find a velocity correction. We update the velocity function and flatten the event. We continue this way, one event at a time. At any given step we have the correct velocity function for the depth of the current event.

We need an equation to find a velocity correction from the observed variation of depth with angle. Modifying the discussion given by Lynn (1979), from

equation (2.3a), when velocity $v(z)$ is correct to depth z, we can write

$$t = \int_0^z \frac{2\, v(\xi)^{-1}}{\left[1 - p^2 v(\xi)^2\right]^{1/2}} d\xi \tag{2.4}$$

For an estimate of velocity $\bar{v}(z)$ the depth will be wrong; denoting this depth by $\bar{z}$ we have

$$t = \int_0^{\bar{z}} \frac{2\, \bar{v}(\xi)^{-1}}{\left[1 - p^2 \bar{v}(\xi)^2\right]^{1/2}} d\xi \tag{2.5}$$

Arrival times are independent of whether we are using the exact or the wrong velocity functions. We can equate equations (2.4) and (2.5) to obtain

$$t = \int_0^z \frac{2\, v(\xi)^{-1}}{\left[1 - p^2 v(\xi)^2\right]^{1/2}} d\xi = \int_0^{\bar{z}} \frac{2\, \bar{v}(\xi)^{-1}}{\left[1 - p^2 \bar{v}(\xi)^2\right]^{1/2}} d\xi \tag{2.6}$$

In a stratified medium, assume that the velocity $\bar{v}$ is correct up to the $(j-1)^{th}$ reflector, *i.e.* $\bar{v}_k = v_k$ for all $k = 1, 2, 3, \ldots, j-1$. If the velocity v_j is constant in the j^{th} interval, we get from equation (2.6)

$$\frac{2\, v_j^{-1}}{\left[1 - p^2 v_j^2\right]^{1/2}} \Delta z_j = \frac{2\, \bar{v}_j^{-1}}{\left[1 - p^2 \bar{v}_j^2\right]^{1/2}} \Delta \bar{z}_j \tag{2.7}$$

where $\Delta z_j = z - z_{j-1}$ and $\Delta \bar{z}_j = \bar{z} - z_{j-1}$. The depth z_{j-1} is the same in both cases because the velocity $\bar{v}$ has been assumed to be correct down to the $(j-1)^{th}$ reflector.

Solving equation (2.7) for v_j we obtain

$$v_j = \left\{ \frac{1}{2p^2} - \frac{1}{2p^2} \left[1 - 4p^2\bar{v}_j^2(1 - p^2\bar{v}_j^2) \left(\frac{\Delta z_j}{\Delta \bar{z}_j} \right)^2 \right]^{1/2} \right\}^{1/2} \qquad (2.8)$$

In this expression we do not know Δz_j. This quantity depends on the velocity $\bar{v}_j$ we are using in the j^{th} interval. We can only approximate it by measuring the depth interval between the $(j-1)^{th}$ and the j^{th} reflectors in (p,z) space when $p = 0$. $\Delta \bar{z}_j$ is the the difference in depth between the $(j-1)^{th}$ reflector and the j^{th} reflector, measured at some non-zero value of p. It can be seen that when we flatten the reflector and the depth becomes independent of p, equation (2.8) gives the true velocity.

The usefulness of this approach is limited because no post-critical energy is used in the estimation. Schultz (1980) estimates velocity using *slant stacks*, which better exploit the sensitivity of post-critical reflections to velocity.

3.3. Transformation to $(\hat{h},\hat{t})$ space.

In this section the problem is to generate a seismic gather from ray-parameter depth space (p,z). From the last section we know that using the correct velocity function makes the data independent of the p coordinate. Velocity information is lost going to (p,z) space. Regenerating the original seismic gather geometry requires the use a replacement velocity $\hat{v}$. In the new gather all events should appear to have the constant replacement velocity.

To obtain the transformation equations we need to replace a constant velocity $\hat{v}$ into equation (2.3) to get

$$\hat{t} = \frac{2z}{\hat{v}\left[1 - p^2\hat{v}^2\right]^{1/2}} \qquad (3.1a)$$

$$\hat{h} = \frac{p\hat{v}z}{\left[1 - p^2\hat{v}^2\right]^{1/2}} \qquad (3.1b)$$

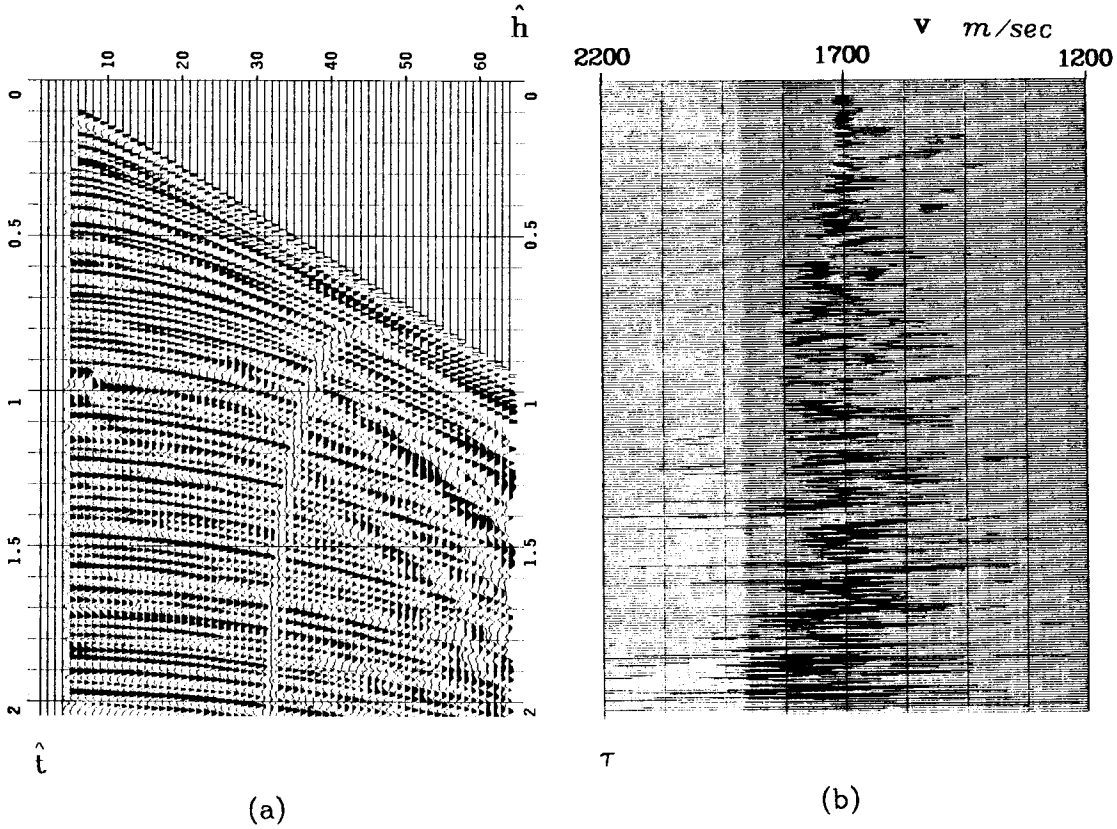

FIGURE 3.1. Marine data in $(\hat{h},\hat{t})$ coordinates. (a) This figure shows the mapping to hyperbolic space for the data of figure (2.2). Since the ray equations used in the transformation can only handle pre–critical reflections, the data was interpolated to duplicate the offset spacing: $dh_{new} = 12.5\,m$. Note the location of the first missing trace from the original and the general hyperbolic look, with few crossing of events. (b) Hyperbolic velocity spectrum. Early arrivals align at $\hat{v}$ because $\bar{v}(z)$ is close to the true velocity. Late arrivals depart from $\bar{v}$, implying we need to correct our original estimate $\bar{v}(z)$.

where $(\hat{t},\hat{h})$ are the new coordinates. Solving these equations for $(p,\,z)$ we get

$$p = \frac{2\hat{h}}{\hat{v}^2\hat{t}} \tag{3.2a}$$

$$z = [\frac{1}{4}\hat{v}^2\hat{t}^2 - \hat{h}^2]^{1/2} \tag{3.2b}$$

This transformation expects the original wavefield to be independent of p. If this is the case, the new wavefield will be hyperbolic. Otherwise it will only be an approximation.

A computer algorithm incorporating the deformation to hyperbolic space does not need to store the intermediate (p, z) space. The ray equations (2.3) are invertible for constant velocity, making possible substitution of equation (3.2) into equation (2.3) and getting the output scanning the input data itself.

Figure (3.1) shows the data from figure (2.2) into hyperbolic space. Since the original data had large offsets, the critical angle for shallow reflections is reached within a few offsets. Mapping the data was thus interpolated to duplicate the sampling spacing in the pre–critical region. This interpolation is easily done while transforming.